Title

Revealing the electronic structure of LiC6 by soft X-ray spectroscopy

Journal

Applied Physics Letters, 110(10)

ISSN

0003-6951

Authors

Zhang, L

Li, X

Augustsson, A

et al.

Publication Date

2017-03-06

DOI

10.1063/1.4978432

Peer reviewed

Revealing the electronic structure of LiC_6 by soft X-ray spectroscopy

L. Zhang, X. Li, A. Augustsson, C. M. Lee, J.-E. Rubensson, J. Nordgren, P. N. RossJr., and J.-H. Guo

Citation: Appl. Phys. Lett. **110**, 104106 (2017); doi: 10.1063/1.4978432
View online: http://dx.doi.org/10.1063/1.4978432
View Table of Contents: http://aip.scitation.org/toc/apl/110/10
Published by the American Institute of Physics

Revealing the electronic structure of LiC_6 by soft X-ray spectroscopy

L. Zhang,[1] X. Li,[2] A. Augustsson,[3] C. M. Lee,[4] J.-E. Rubensson,[3] J. Nordgren,[3] P. N. Ross, Jr.,[4] and J.-H. Guo[1,5,a)]

[1]*Advanced Light Source, Lawrence Berkeley National Laboratory, Berkeley, California 94720, USA*
[2]*Hefei National Laboratory for Physical Sciences at the Microscale, University of Science and Technology of China, Hefei, Anhui 230026, People's Republic of China*
[3]*Department of Physics, Uppsala University, Box 530, S-75121 Uppsala, Sweden*
[4]*Materials Science Division, Lawrence Berkeley National Laboratory, Berkeley, California 94720, USA*
[5]*Department of Chemistry and Biochemistry, University of California at Santa Cruz, Santa Cruz, California 95064, USA*

(Received 24 December 2016; accepted 28 February 2017; published online 9 March 2017)

The electronic structure of LiC_6 has been investigated by soft X-ray absorption and emission spectroscopies. The results reveal that upon full lithiation of graphite, the Li 2s electrons are transferred into the carbon π^* states in a near rigid-band behavior, resulting in the increased density of states near E_F and the shift of σ^* states to lower energies. In addition, the resonant inelastic X-ray scattering spectra of LiC_6 do not show strong dispersive features as that of graphite, indicating that the crystal momentum is not conserved during the scattering process due to the delocalization of electrons in the intermediate state. *Published by AIP Publishing.* [http://dx.doi.org/10.1063/1.4978432]

Lithium-ion batteries (LIBs) are the primary power source for portable electronic application.[1,2] The commercial LIBs usually use carbonaceous materials as the negative electrode. Among the various carbonaceous materials, graphite is most attractive mainly because of its low cost, relatively high energy density, and long durability.[3,4] The lithiation and dilithiation processes of graphite have been characterized extensively and it is found that various complex compounds exist for the Li-intercalated graphite anode at different stages, including LiC_6, LiC_{12}, LiC_{18}, and LiC_{24}.[5,6] At the stage of full lithiation, graphite and Li form a stable structure with the highest in-plane density of Li, namely, LiC_6. In addition, the stacking order of graphene layers shifts from AB to AA stacking and the distance between neighboring layers increases by 10.3% upon full lithiation.[6]

The electronic properties of LiC_6 have also been investigated both experimentally[7–12] and theoretically.[13,14] It is believed that upon lithiation, the density-of-states (DOS) of graphite remains largely unchanged and the Li 2s electrons are completely transferred to the carbon π^* orbitals.[7–11] However, the influence of full lithiation on the electronic band structure of graphite is still not fully understood, mainly due to the extreme sensitivity of LiC_6 to oxygen together with the surface sensitivity of the relevant spectroscopic techniques.[7,8] Therefore, a systematic study is highly desirable to acquire more fundamental understandings of the lithiation mechanism and guidelines for the optimization of carbonaceous electrode materials in LIBs.

Soft X-ray absorption spectroscopy (XAS), soft X-ray emission spectroscopy (XES), and resonant inelastic X-ray scattering (RIXS) have been proved to be powerful techniques for investigating the electronic structure of carbon allotropes.[15–17] Specifically, the RIXS process conserves the crystal momentum and hence provides a way for obtaining symmetry-resolved band structure information, which has already been applied to diamond,[15] graphite,[16] and graphene.[17] The above-mentioned spectroscopies have intrinsic bulk sensitivity due to the comparatively large photon attenuation lengths. In the present work, we have employed XAS, XES, and RIXS to investigate the influence of full lithiation on both valence band and conduction band structures of graphite.

The experiments were performed on the undulator beamline 8.0.1 at Advanced Light Source, Lawrence Berkeley National Laboratory. The XAS spectra were collected by both surface-sensitive total electron yield (TEY, probing depth of about 5 nm) and bulk-sensitive total fluorescent yield (TFY, probing depth of about 100 nm). All spectra were normalized to the photocurrent from a clean gold mesh introduced upstream the sample into the beam. A grazing-incidence grating spectrometer was used to record the XES and RIXS spectra with a resolution better than 0.3 eV. The bandpass of photon beam was set to 0.1 eV for absorption and 0.3 eV for emission measurements. The base pressure of the ultra-high-vacuum (UHV) chamber for the experiment was 5×10^{-10} mbar.

A large ($10 \times 10\,mm^2$) highly oriented pyrolytic graphite (HOPG) sample was cleaved using an adhesive tape to obtain a fresh surface prior loading it in the vacuum chamber. The LiC_6 sample was prepared by exposing HOPG to Li vapor in a UHV chamber.[18] The sample was then brought to the beamline in a sealed container and introduced into the UHV system via a load lock with a glove bag under argon atmosphere. The sample was cleaved immediately before loaded into the chamber. The LiC_6 sample kept its characteristic golden color throughout the experiment time (~12 h).

Figure 1 shows the polarization-dependent C K-edge XAS spectra of LiC_6 in both TEY (a) and TFY (b) modes with grazing and normal incidence, respectively. The corresponding spectra of HOPG are also shown as reference. In the XAS process, electrons are excited from a C K-shell into π^* or σ^* states depending on the orientation of the incident

a)Electronic mail: jguo@lbl.gov

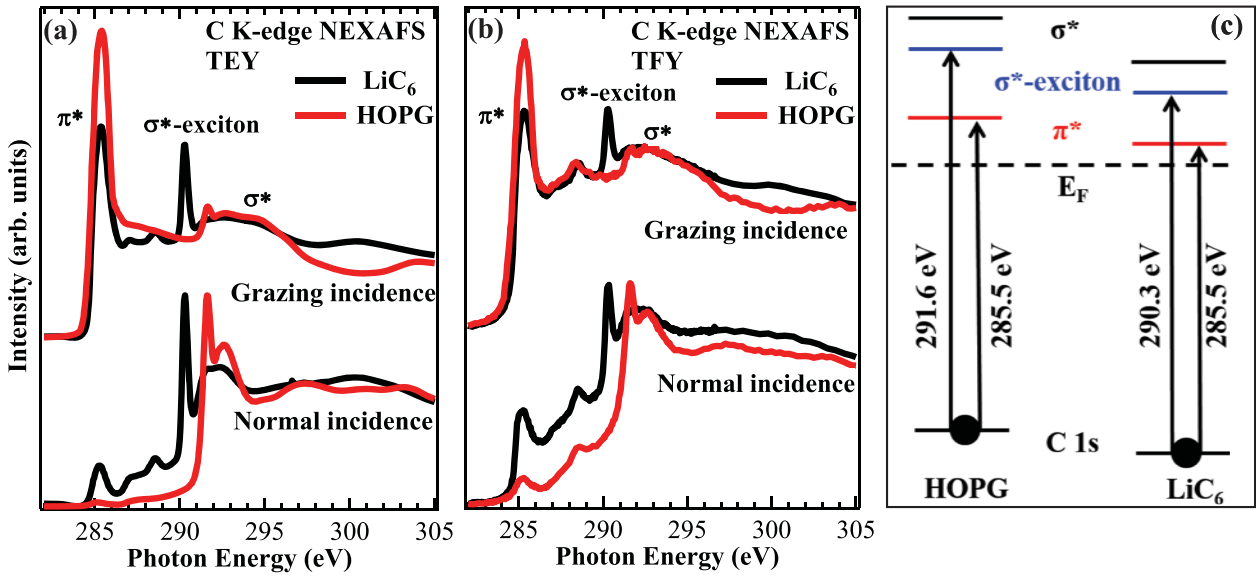

FIG. 1. Polarization-dependent C K-edge XAS spectra of LiC_6 and HOPG in surface-sensitive TEY with a probing depth of about 5 nm (a) and bulk-sensitive TFY with a probing depth of about 100 nm (b), respectively. (c) The schematic illustration of the energy level of HOPG and LiC_6. Note that the C 1s core level of LiC_6 shifts to higher binding energy due to the charge transfer from Li to HOPG.[18]

photon polarization vector with respect to the graphite basal plane. The XAS spectra of HOPG with grazing incidence show a strong π^* peak at 285.5 eV and a broad σ^* peak at 292.6 eV, which is in good agreement with the previous reports.[16,19] In addition, by comparing the grazing- and normal-incidence XAS spectra, it is clear that both π^* and σ^* features show a strong dichroism due to the high alignment of HOPG.[16,19] The sharp feature at 291.6 eV is attributed to σ^*-exciton state.[20] The feature located at 288.5 eV in TFY spectra but absent in TEY spectra originates from the three-dimensional interlayer state as revealed by recent experiments and theoretical calculations.[21]

For the XAS spectra of LiC_6 at grazing incidence, the intensity of π^* states decreases compared with that of HOPG, signaling the charge transfer from Li 2s states to carbon π^* states.[9,11,12] A similar phenomenon was also observed before in the C K-edge electron energy-loss spectroscopy (EELS) of LiC_6; however, the Li K-edge EELS spectra of metallic Li and LiC_6 are nearly identical, indicating a small charge transfer from Li to carbon in LiC_6.[22] The dichroism of π^* and σ^* states in the XAS spectra of LiC_6 is also kept. However, the π^* states do not vanish when the incident beam is normal to the surface, indicating the warping of HOPG due to full lithiation.[19] In addition, the σ^*-exciton state is shifted by ~1.3 eV towards lower energy, while no peak shift is observed for the π^* state (Figure 1(c)). The shift of exciton state was also observed before for nanodiamond thin films with different grain diameters and was explained by the presence of a quantum confinement effect.[23] As there is no such effect in LiC_6, the shift of σ^*-exciton state is explained by the increase of the C-C bond length in LiC_6 due to the charge transfer from Li to π band of HOPG (the C-C bond length of LiC_6 is ~0.15 Å longer than that of graphite).[6,24,25] The downward shift of the σ^* state was also observed earlier in the C 1s hard X-ray non-resonant inelastic X-ray scattering of LiC_6.[11]

The features located between π^* and σ^* states of LiC_6 are induced by the orbital hybridization between Li and HOPG. Similar features were also found in the C K-edge XAS spectrum of graphene on Ru(0001) as a result of the strong covalent bonding between graphene and Ru(0001).[24] Note that C-O contamination can also result in the appearance of these features.[26] However, no such feature is observed in the surface-sensitive TEY spectra of HOPG, indicating that the C-O contamination gives negligible contribution to the XAS feature at this energy. It is worth mentioning that the TFY spectra of both HOPG and LiC_6 are slightly different from the corresponding TEY spectra, which originates from the saturation effects as the photon detector only covers a small solid angle of the out-going photons.

The RIXS spectra of LiC_6 with different excitation energies, along with the corresponding spectra of HOPG, are shown in Figure 2. These emission spectra were collected with the incident angle of 40° from the surface normal. For comparison, the non-resonant XES spectra with the excitation energy of 320.0 eV are also shown.

The non-resonant XES spectrum directly reflects the PDOS of the investigated material.[15,16] Compared with HOPG, the spectrum of LiC_6 shows some intensity modulation at ~281.5 eV and ~274.8 eV, which is mainly attributed to the charge transfer and the change in the band structure.[19] In addition, the appearance of a strong peak at ~284.0 eV indicates the increased DOS near E_F for LiC_6. Earlier published C K-edge XES spectrum of LiC_6 also shows an enhanced feature near E_F.[9] However, the spectrum was measured by using high energy electron excitation and was corrected for "radiative auger emission" with only the π contribution.[9]

For the RIXS spectra, the strong emission peak located at high emission energy is the elastic peak, which shifts to higher emission energy with increasing the excitation energy. The assignment of the inelastic features is achieved by comparing with the calculated band structure of LiC_6.[13] Angle-resolved RIXS spectra were also recorded to determine the π or the σ character of the emission features, as shown in Figure 3. The intensity variation of the emission

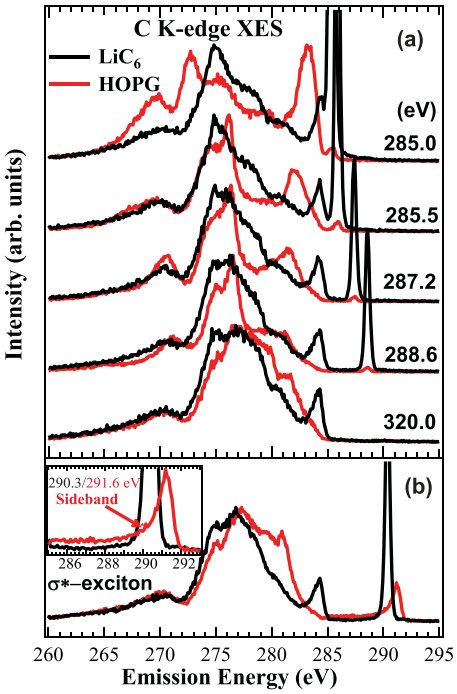

FIG. 2. (a) RIXS and non-resonant XES spectra of LiC_6 and HOPG. (b) RIXS spectra of LiC_6 and HOPG with the excitation energy at σ^*-exciton state. The inset shows the comparison of the RIXS spectra near elastic peak.

features with the emission angle is due to the difference in the intensity distribution between π and σ states. For example, if the incident angle is close to 90°, the enhancement of π states should be observed (e.g., $\theta = 80°$), while at the grazing-incidence angle, the π states will be suppressed (e.g., $\theta = 15°$). From the intensity variation of the emission spectra in Figure 3, it is clear that the peak at ~284.0 eV and the broad features at ~280.4 and ~274.8 eV have π symmetry, whereas the features at ~277.0 eV and ~270.5 eV have σ symmetry. The π characteristics of the feature at ~284.0 eV confirm that the electrons transferred from Li are mainly located on the π orbital of HOPG.[10,11] In order to compare

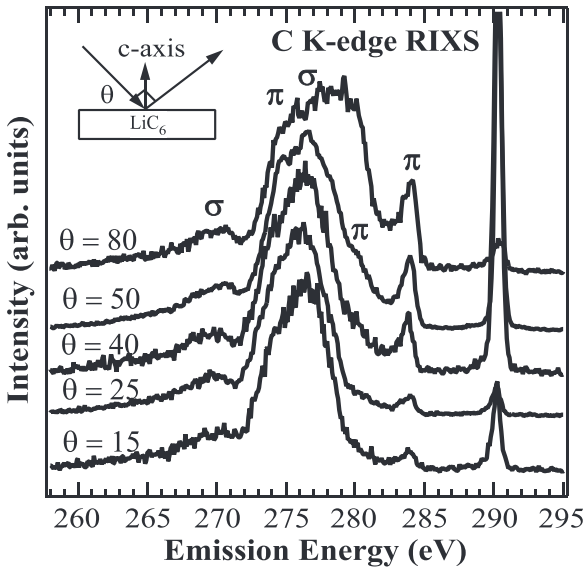

FIG. 3. RIXS spectra of LiC_6 recorded with different incident angles (θ). The excitation energy is 290.3 eV (σ^*-exciton state).

the emission data with theory, we have defined the relative position of E_F to C 1s to be 284.4 eV as determined by the intersection position of XAS and XES spectra, which is in good agreement with the value reported before.[7]

The comparison of energy positions of π and σ states among XES, photoemission (PES), and calculated band structure is demonstrated in Table I. The position of lower energy bands fits quite well with theory and PES results. However, the position of upper π band at C point from XES and PES (−0.5 eV) is closer to E_F than the value predicted by theory (−1.3 eV). This observation indicates that the valence band close to E_F does not shift according to the rigid-band model as a consequence of the substantial hybridization between Li 2s states and carbon π^* states.[7]

Returning now to the RIXS spectra in Figure 2(a), it is obvious that the RIXS spectral shape of LiC_6 is different from that of HOPG. The RIXS spectra of HOPG at different excitation energies show strong dispersive features, which can be directly related to the band structure of graphite due to the conservation of the crystal momentum during the scattering process.[16,17] However, no such dispersive features are observed for LiC_6, indicating that the rule of crystal momentum conservation in the scattering process is not valid for LiC_6. In addition, the absence of emission peaks related to the C-O species in the RIXS spectra of LiC_6 further confirms that the XAS features between π^* and σ^* states originate from the orbital hybridization between Li and HOPG rather than C-O contamination.[19,27]

In fact, although the crystal structure of graphite changes moderately upon lithiation, the long-range crystallographic order is still kept and the crystal momentum of LiC_6 should be conserved in the scattering process as it does in graphite.[6] However, it is possible that there exist some local C-C bond distortions in LiC_6, which result in the lack of dispersive features in the RIXS spectra. In addition, the increased DOSs near E_F can also affect the coherence in the scattering process: the excited electrons are delocalized and the coherence fraction is decreased due to the enhanced electron-electron interactions in the intermediate state.[15] A closer inspection of the σ^*-exciton state RIXS spectra (Figure 2(b)) gives us further clues. Ma *et al.* have found that for the RIXS spectra of graphite, there is a recombination peak near the excitation energy with a long phonon tail, which is similar to our results here.[28] The presence of the phonon sideband in the emission spectrum suggests that there is a strong vibronic coupling effect in graphite due to a large Jahn-Teller relaxation of the

TABLE I. Comparison of the energy positions between experiment and theory for LiC_6.

Symmetry	XES (eV)	PES[a] (eV)	Theory[b] (eV)
π (C)	−0.5	−0.5	−1.3
π (M)	−4	…	−4
σ (C)	−6	−5.5	−5.9
π (C)	−9.6	−9.3	−9.3
σ (C)	−13.8	−13	−13.3

[a]The energy positions of C- and M-point are derived from Ref. 8 (photoemission).
[b]The energy positions of C- and M-point are derived from Ref. 13 (theory).

excited carbon atom within the core hole lifetime.[28] For graphite, this side-band is readily observed, while for LiC_6 there is almost no intensity in that region (see inset in Figure 2(b)). This again points towards the delocalization of the electrons in the intermediate state within the core hole lifetime of excited carbon in LiC_6.

To conclude, we have investigated the electronic structure of LiC_6 using XAS, XES, and RIXS. The XAS spectra of LiC_6 show a shift of σ^* states to lower energy by 1.3 eV, while no shift is observed for the π^* states. This observation is understood as a consequence of the charge transfer from Li 2s states to π^* states of graphite in a near rigid-band behavior. In addition, no strong dispersive features are observed in the RIXS spectra of LiC_6, indicating that the crystal momentum is not conserved during the scattering process as that of HOPG. This originates from the delocalization of the excited electrons in the intermediate state and thus less coherent fraction in the RIXS spectra. Our present study clearly demonstrates that XAS and XES are effective methods for clarifying the electronic properties of LiC_6, which could provide valuable information for further designing the carbonaceous electrode materials.

The Advanced Light Source was supported by the Director, Office of Science, Office of Basic Energy Sciences, of the U.S. Department of Energy under Contract No. DE-AC02-05CH11231.

[1]D. Larcher and J.-M. Tarascon, Nat. Chem. **7**, 19 (2015).
[2]J.-M. Tarascon and M. Armand, Nature **414**, 359 (2001).
[3]B. Scrosati and J. Garche, J. Power Sources **195**, 2419 (2010).
[4]J. B. Goodenough and K. S. Park, J. Am. Chem. Soc. **135**, 1167 (2013).
[5]V. A. Sethuraman, L. J. Hardwick, V. Srinivasan, and R. Kostecki, J. Power Sources **195**, 3655 (2010).
[6]M. Winter, J. O. Besenhard, M. E. Spahr, and P. Novak, Adv. Mater. **10**, 725 (1998).
[7]W. Scheelke, A. Berthold, A. Kaprolat, and H.-J. Gentherodt, Phys. Rev. Lett. **60**, 2217 (1988).
[8]W. Eberhardt, I. T. McGovern, E. W. Plummer, and J. E. Fisher, Phys. Rev. Lett. **44**, 200 (1980).
[9]A. Mansour, S. E. Schnatterly, and J. J. Ritsko, Phys. Rev. Lett. **58**, 614 (1987).
[10]Z.-H. Pan, J. Camacho, M. H. Upton, A. V. Fedorov, C. A. Howard, M. Ellerby, and T. Valla, Phys. Rev. Lett. **106**, 187002 (2011).
[11]M. Balasubramanian, C. S. Johnson, J. O. Cross, G. T. Seidler, T. T. Fister, E. A. Stern, C. Hamner, and S. O. Mariager, Appl. Phys. Lett. **91**, 031904 (2007).
[12]J. Langer, V. Epp, P. Heigjans, F. A. Mautner, and M. Wilkening, Phys. Rev. B **88**, 094304 (2013).
[13]N. A. Holzwarth, S. Rabii, and L. A. Girifalco, Phys. Rev. B **18**, 5190 (1978).
[14]Y. Z. Lin, T. A. Strobel, and R. E. Cohen, Phys. Rev. B **92**, 214106 (2015).
[15]Y. Ma, N. Wassdahl, P. Skytt, J. Guo, J. Nordgren, P. D. Johnson, J. E. Rubensson, T. Boske, W. Eberhardt, and S. D. Kevan, Phys. Rev. Lett. **69**, 2598 (1992).
[16]P. Skytt, P. Glans, D. C. Mancini, J.-H. Guo, N. Wassdahl, J. Nordgren, and Y. Ma, Phys. Rev. B **50**, 10457 (1994).
[17]L. Zhang, N. Schwertfager, T. Cheiwchanchamnangij, X. Li, P.-A. Glans-Suzuki, L. F. J. Piper, S. Limpijumnong, Y. Luo, J. F. Zhu, W. R. L. Lambrecht, and J.-H. Guo, Phys. Rev. B **86**, 245430 (2012).
[18]C.-M. Lee, B.-J. Mun, and P. N. Ross, Jr., J. Electrochem. Soc. **149**, A1286 (2002).
[19]L. Zhang, E. Pollak, W.-C. Wang, P. Jiang, P.-A. Glans, Y. G. Zhang, J. Cabana, R. Kostecki, C.-L. Chang, M. Salmeron *et al.*, Carbon **50**, 5316 (2012).
[20]P. A. Brühwiler, A. J. Maxwell, C. Puglia, A. Nilsson, S. Andersson, and N. Mårtensson, Phys. Rev. Lett. **74**, 614 (1995).
[21]V. N. Strocov, P. Blaha, H. I. Starnberg, M. Rohlfing, R. Claessen, J.-M. Debever, and J.-M. Themlin, Phys. Rev. B **61**, 4994 (2000).
[22]A. Hightower, C. C. Ahn, B. Fultz, and P. Rez, Appl. Phys. Lett. **77**, 238 (2000).
[23]Y. K. Chang, H. H. Hsieh, W. F. Pong, M.-H. Tsai, F. Z. Chien, P. K. Tseng, L. C. Chen, T. Y. Wang, K. H. Chen, D. M. Bhusari *et al.*, Phys. Rev. Lett. **82**, 5377 (1999).
[24]A. B. Preobrajenski, M. L. Ng, A. S. Vinogradov, and N. Mårtensson, Phys. Rev. B **78**, 073401 (2008).
[25]J. Stöhr, *NEXAFS Spectroscopy* (Springer, Heidelberg, 1992).
[26]M. Abbas, Z. Y. Wu, J. Zhong, K. Ibrahim, A. Fiori, S. Orlanducci, V. Sessa, M. L. Terranova, and I. Davoli, Appl. Phys. Lett. **87**, 051923 (2005).
[27]G. Abrasonis, M. Berndt, M. Krause, K. Kuepper, F. Munnik, A. Kolitsch, and W. Möller, J. Phys. Chem. C **112**, 17161 (2008).
[28]Y. Ma, P. Skytt, N. Wassdahl, P. Glans, D. C. Mancini, J. Guo, and J. Nordgren, Phys. Rev. Lett. **71**, 3725 (1993).